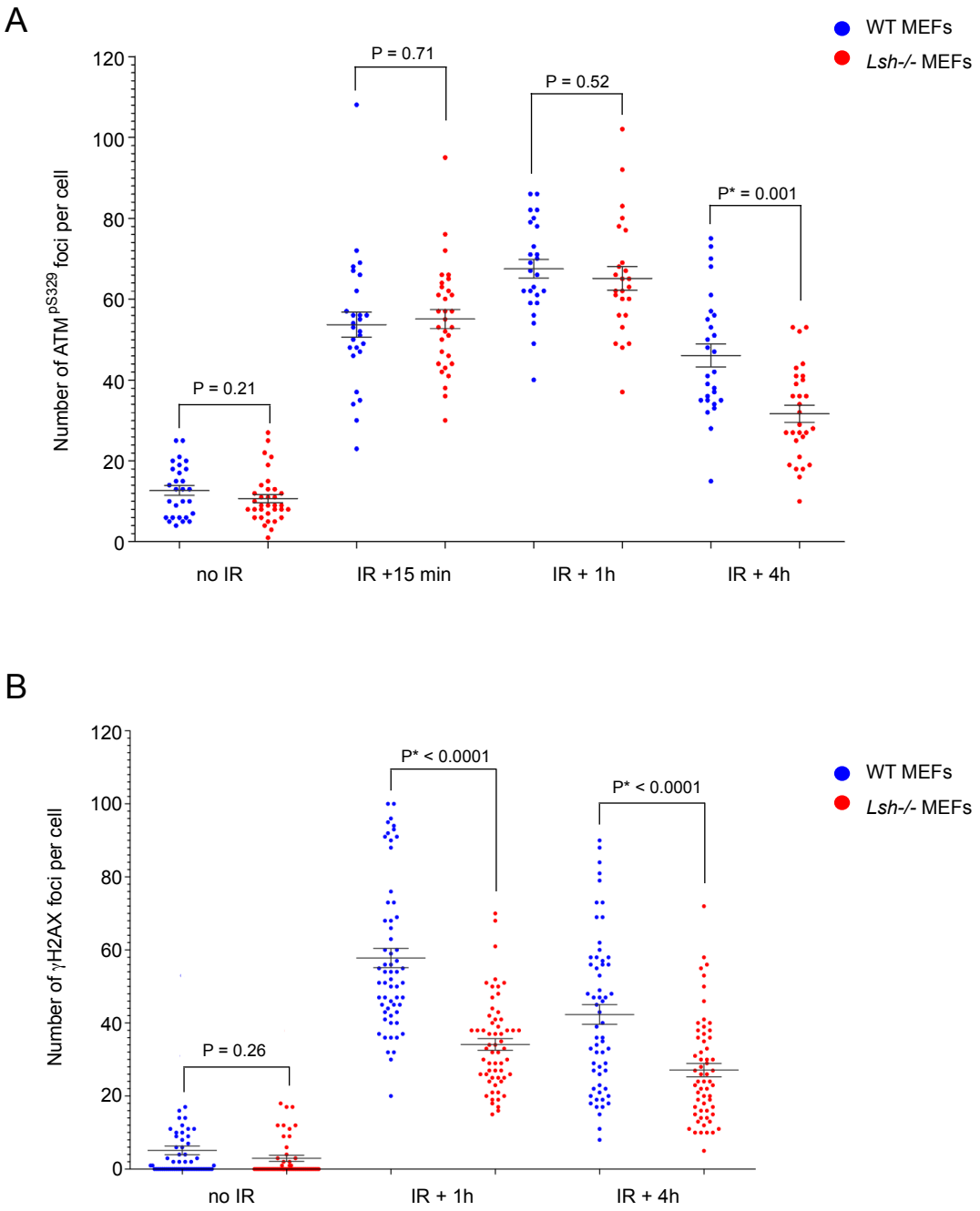

Supplemental Figure 1 Quantification of ATM^{pS329} and γH2AX foci in wild-type and *Lsh-/-* MEFs

A. Counts of ATM^{pS329} foci in non-irradiated and irradiated wild-type and *Lsh-/-* MEFs at indicated time points. Each dot on the graph represents a single cell. The mean value and the standard error of the mean are indicated for each group of cells. Note that there is no significant difference between the wild-type and *Lsh-/-* cells in the number of ATM^{pS329} foci observed 15 minutes and 1 hour post-IR indicating that the initial recognition of DSBs is not impaired in LSH-deficient cells. Comparable number of foci also correlates well with equal amount of DNA damage induced by IR in both cell lines as quantified by the comet assays in Figure 1D. However, the number of ATM^{pS329} foci are significantly reduced in *Lsh-/-* MEFs 4 hours after IR. This is consistent with reduced γH2AX levels in *Lsh-/-* MEFs at this time point and the existence of a feed back loop at later time points after DNA damage where spreading of γH2AX from the break recruits more ATM in MDC1/MRN-dependent manner allowing continuous ATM signalling at slow repairing breaks (Lou et al, 2006; van Atticum and Gasser, 2009).

B. Counts of γH2AX foci in wld-type and *Lsh-/-* MEFs. The mean value and the standard error are indicated. Note that *Lsh-/-* MEFs show reduced number of foci at 1h and 4h time points after IR, which is consistent with the reduced signal observed in Western blots.

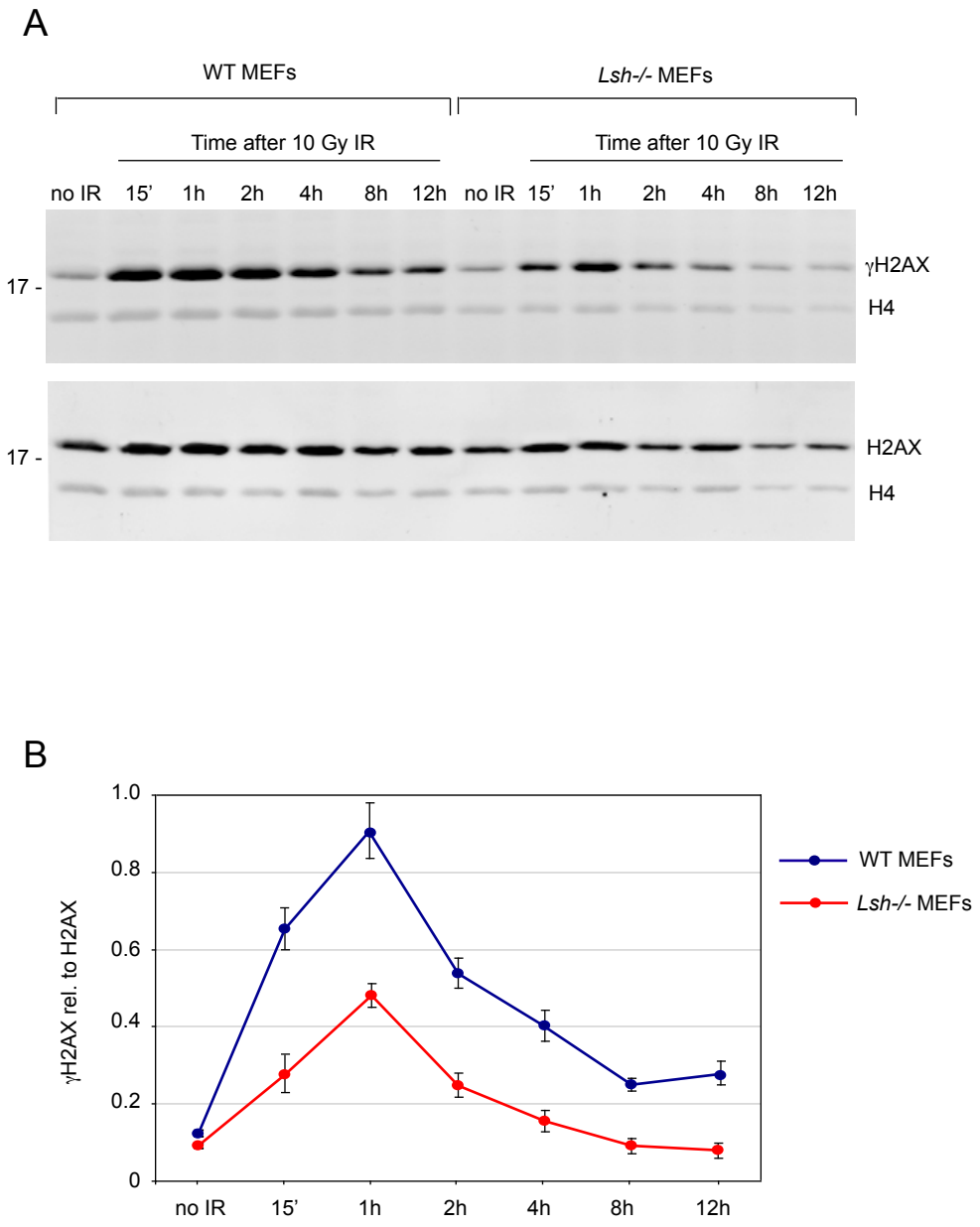

Supplemental Figure 2 Inefficient phosphorylation of H2AX in irradiated *Lsh-/-* MEFs

A. A representative quantitative Western blot detecting γH2AX, H2AX and histone H4 in nuclear extracts of wild type and *Lsh-/-* MEFs before and after exposure to 10Gy of ionizing radiation. Irradiated MEFs were collected at indicated time points.

B. Average levels of γH2AX relative to H2AX in wild-type and *Lsh-/-* MEFs during recovery from IR quantified from Western blots representing three independent experiments (biological replicates). Note that *Lsh-/-* MEFs do not display reduced levels of H2AX. Histone H4 serves as endogenous loading control.

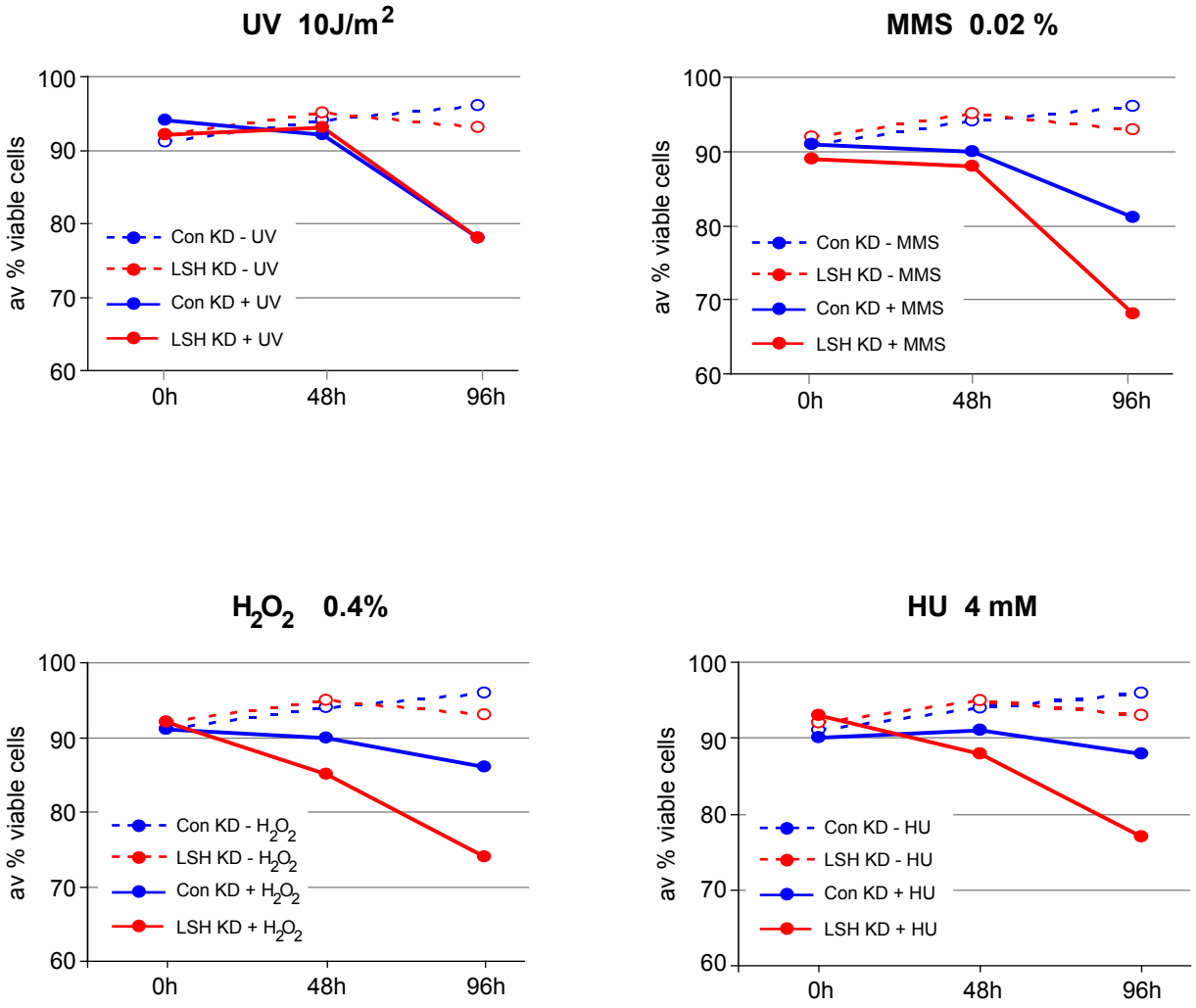

Supplemental Figure 3 Sensitivity of control and LSH-deficient MRC5 cells to DNA damaging agents

Control MRC5 cells expressing non-silencing shRNA and LSH KD MRC5 cells were tested for viability after treatment with UV, MMS, hudroxyurea (HU) and hydrogen peroxide (H_2O_2). Note that LSH KD cells are more sensitive to most DNA damaging agents, but not UV or camptothecin (not shown). The % viable cells was determined as described in Figure 7D.

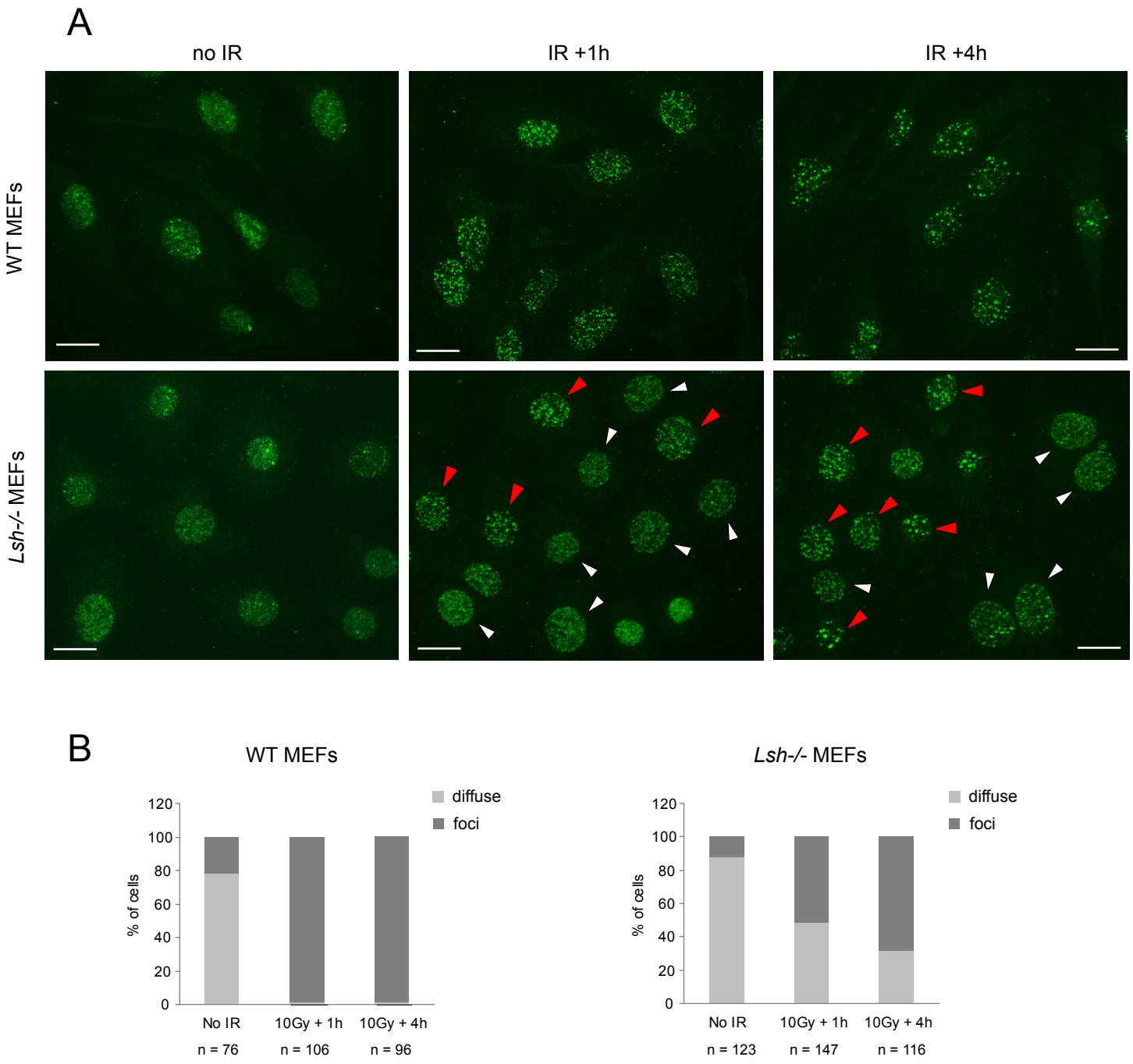

Supplemental Figure 4 Localization of 53BP1 in wild type and *Lsh-/-* MEFs

A. Representative images of wild type and *Lsh-/-* MEFs before and after IR (1- and 4-hour time points) stained with antibodies against 53BP1. In the panels showing irradiated *Lsh-/-* MEFs cells the white arrows indicate cells with diffuse 53BP1 staining and the red arrows point to cells that form discrete 53BP1 foci. The scale bar represents 10 μm

B. Quantification of cells with diffuse and punctated 53BP1 staining. "n" indicates the number of cells counted at each time point.

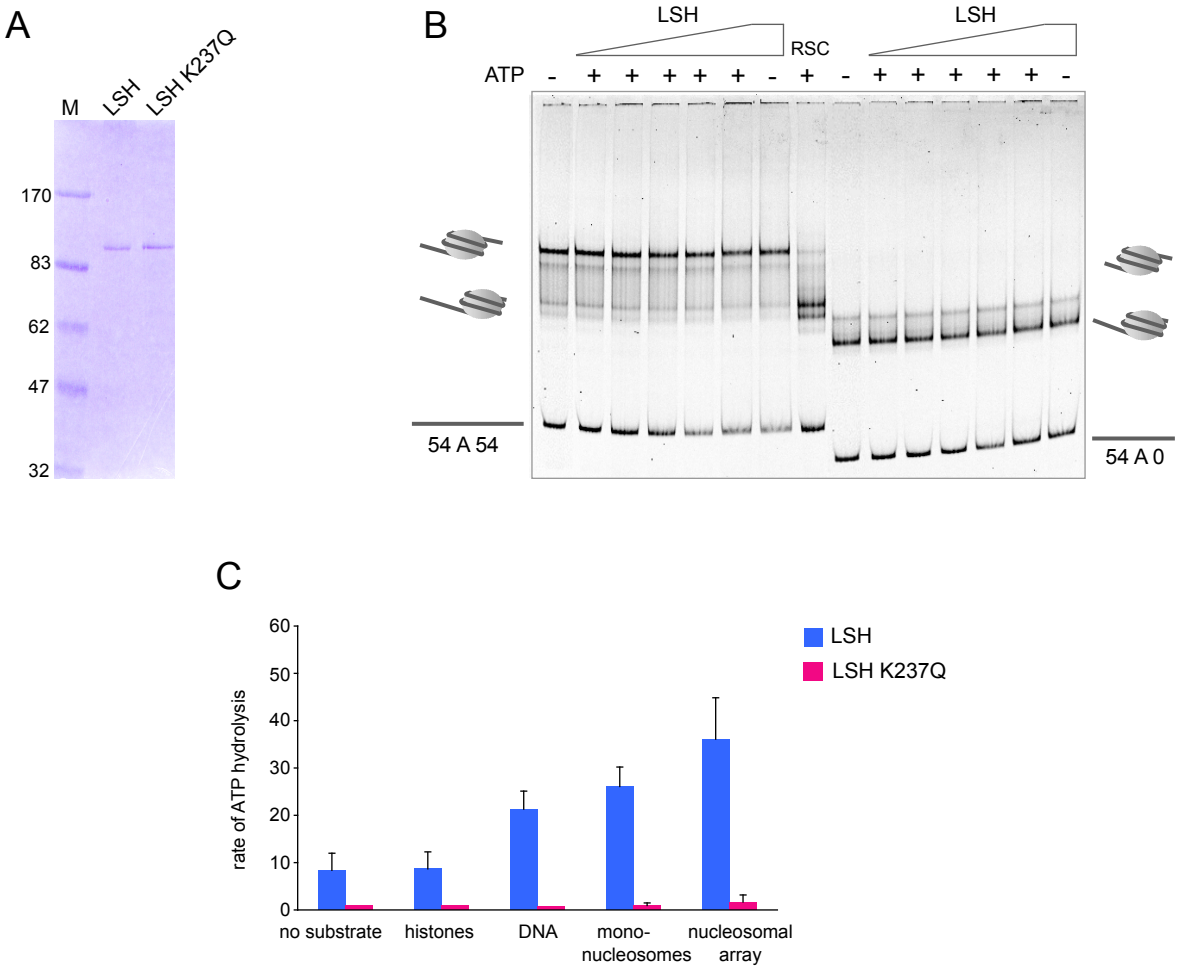

Supplemental Figure 5 Nucleosome repositioning and ATPase activity of recombinant LSH

A. Recombinant wild type and mutant 6xHis-tagged LSH proteins were expressed in insect cells and purified by Ni-affinity chromatography followed by ion exchange chromatography to remove any LSH-bound DNA. M represents molecular weight marker.

B. Recombinant wild type LSH does not reposition either a centrally (54A54) or end positioned nucleosome (54A0) in the presence of ATP. Recombinant yeast RSC protein (100 nM) was used as a control protein that repositions a centrally positioned nucleosome. The triangles indicate increasing concentrations of LSH protein in the reaction (25, 50, 100, 200, 300 nM).

C. LSH shows a weak DNA-stimulated ATPase activity, which is disrupted by the K237Q mutation in ATP binding site. The rate of ATP hydrolysis represents molecules ATP hydrolysed per minute per mol LSH.

Table S1. Expression of DNA repair genes in wild-type and *Lsh-/-* MEFs

The table contains an extract of expression microarray data from Myant et al (2011) *Genome Res* **21**, 83-94 comparing the wild-type (WT) and *Lsh-/-* (KO) MEFs.

M.KO = log2(KO-WT)
FDR.KO = false discovery rate, after p-value adjustment for multiple testing (Benjamini-Hochberg method)
KO = log2(KO)
WT = log2 (WT)

Chr	Gene Name	Gene_ID	Description	M.KO	FDR.KO	KO	WT	Fold change
chr9	H2afx	15270	\H2A histone family, member X\""	-0.2	0.071	13.1	13.0	0.9
chr9	Mre11a	17535	meiotic recombination 11 homolog A (S. cerevisiae)	-0.5	0.052	11.9	12.4	0.7
chr11	Rad50	19360	RAD50 homolog (S. cerevisiae)	-0.1	0.658	12.9	13.0	0.9
chr4	Nbn	27354	nibrin	-0.1	0.573	12.5	12.7	0.9
chr15	Xrcc6 (Ku70)	14375	X-ray repair complementing defective repair in Chine	-0.7	0.013	12.3	12.9	0.6
chr1	Xrcc5 (Ku80)	22596	X-ray repair complementing defective repair in Chine	-0.2	0.551	12.7	12.9	0.9
chr9	Atm	11920	ataxia telangiectasia mutated homolog (human)	-0.3	0.135	11.3	11.5	0.8
chr9	Atr	235533	ataxia telangiectasia and Rad3 related	-0.1	0.743	8.4	8.6	0.9
chr16	Prkdc	19090	\protein kinase, DNA activated, catalytic polypeptide\	0.6	0.008	11.8	11.1	1.5
chr18	Rbbp8 (CtIP)	225182	retinoblastoma binding protein 8	-0.6	0.039	8.9	9.4	0.7
chr1	Exo1	26909	exonuclease 1	-0.5	0.114	8.8	9.3	0.7
chr7	Blm	12144	Bloom syndrome homolog (human)	-1.2	0.000	11.3	12.4	0.4
chr5	Xrcc2 Rad51	57434	X-ray repair complementing defective repair in Chine	-1.1	0.002	8.4	9.5	0.5
chr11	Rad51c	114714	Rad51 homolog c (S. cerevisiae)	-0.4	0.083	7.6	8.0	0.8
chr12	Rad51l1	19363	RAD51-like 1 (S. cerevisiae)	-0.2	0.769	7.5	7.7	0.9
chr11	Rad51l3	19364	RAD51-like 3 (S. cerevisiae)	-0.2	0.626	7.5	7.8	0.9
chr11	Rpa1	68275	replication protein A1	-0.5	0.041	12.2	12.5	0.7
chr6	Rad52	19365	RAD52 homolog (S. cerevisiae)	-0.3	0.153	11.6	11.9	0.8
chr9	Rad54l2	81000	Rad54 like 2 (S. cerevisiae)	0.4	0.102	10.4	10.1	1.3
chr4	Rad54l	19366	RAD54 like (S. cerevisiae)	-0.7	0.011	12.3	13.0	0.6
chr17	Mdc1	240087	mediator of DNA damage checkpoint 1	0.2	0.004	9.8	9.6	1.1
chr19	Rad9 (53BP1)	19367	RAD9 homolog (S. pombe)	-0.3	0.020	12.8	13.0	0.8
chr2	Dclre1c (Atrtemis)	227525	\DNA cross-link repair 1C, PSO2 homolog (S. cerevis	0.0	0.983	7.9	8.0	1.0
chr13	Xrcc4 (Ligase IV)	108138	X-ray repair complementing defective repair in Chine	0.0	0.889	9.9	10.0	1.0
chr7	Xrcc1 DNA lig3	22594	X-ray repair complementing defective repair in Chine	-0.5	0.033	12.6	13.1	0.7
chr12	Xrcc3 HJ resolvase	74335	X-ray repair complementing defective repair in Chine	0.3	0.219	10.2	9.9	1.3
chr15	Rad1	19355	RAD1 homolog (S. pombe)	0.0	0.941	11.3	11.3	1.0
chr15	Rad21	19357	RAD21 homolog (S. pombe)	0.0	0.983	14.0	13.9	1.0
chr13	Rad17	19356	RAD17 homolog (S. pombe)	-0.2	0.420	12.4	12.6	0.9
chr9	Rad54l2	81000	Rad54 like 2 (S. cerevisiae)	0.4	0.102	10.4	10.1	1.3
chr8	Rad23a	19358	RAD23a homolog (S. cerevisiae)	0.6	0.007	13.5	13.0	1.5
chr6	Rad18	58186	RAD18 homolog (S. cerevisiae)	-0.8	0.002	11.1	11.9	0.6
chr5	Rad9b	231724	RAD9 homolog B (S. cerevisiae)	0.7	0.059	7.3	6.7	1.6
chr4	Rad54l	19366	RAD54 like (S. cerevisiae)	-0.7	0.011	12.3	13.0	0.6
chr4	Rad23b	19359	RAD23b homolog (S. cerevisiae)	-0.3	0.245	14.3	14.5	0.8
chr6	Rad52	19365	RAD52 homolog (S. cerevisiae)	-0.3	0.153	11.6	11.9	0.8
chr11	Brca1	12189	breast cancer 1	-0.2	0.001	11.8	11.7	0.9
chr5	Brca2	12190	breast cancer 2	-0.3	0.002	11.0	11.3	0.8
								1.0
chr9	Chek1 (Rad27)	12649	checkpoint kinase 1 homolog (S. pombe)	-0.2	0.000	9.7	9.9	0.9
chr5	Chek2 (Rad53)	50883	CHK2 checkpoint homolog (S. pombe)	-0.9	0.003	8.7	9.6	0.6
chr11	Trp53	22059	transformation related protein 53	0.9	0.002	13.8	12.9	1.9
chr19	Htatip (Tip60)	81601	\HIV-1 tat interactive protein, homolog (human)\""	-0.1	0.821	12.6	12.6	1.0
chr7	Htatip2	53415	\HIV-1 tat interactive protein 2, homolog (human)\""	0.4	0.002	7.8	7.4	1.4
chr19	Ddb1	13194	damage specific DNA binding protein 1	-0.2	0.397	14.8	15.0	0.9
chr2	Ddb2	107986	damage specific DNA binding protein 2	0.5	0.103	10.1	9.7	1.4
chr8	Cul4a	99375	cullin 4A	-0.5	0.031	13.4	13.9	0.7
chrX	Cul4b	72584	cullin 4B	-0.3	0.148	13.1	13.5	0.8
chr17	Rnf8	58230	ring finger protein 8	-0.8	0.003	11.5	12.2	0.6
chr16	Rnf168	70238	ring fnger protein 168	0.0	0.967	10.6	10.6	1.0
chr1	Smarcal1	54380	\Swi/SNF related matrix associated, actin dependent	0.5	0.092	10.7	10.3	1.4
chr2	Inoc1 (Ino80)	68142	INO80 complex homolog 1 (S. cerevisiae)	0.1	0.871	11.1	11.0	1.0
chr3	Smarca3 Hltf	20585	\SWI/SNF related, matrix associated, actin depender	-1.2	0.000	9.9	11.1	0.4
chr3	Smarca3	20585	\SWI/SNF related, matrix associated, actin depender	-0.9	0.002	7.6	8.6	0.5
chr3	Chd1l (ALC1)	68058	chromodomain helicase DNA binding protein 1-like	-1.5	0.000	10.9	12.3	0.3
chr6	Smarcad1	13990	\SWI/SNF-related, matrix-associated actin-depender	-0.5	0.051	10.5	10.9	0.7
chr8	Smarca5 Snf2h , WCRF13	93762	\SWI/SNF related, matrix associated, actin depender	-0.5	0.059	13.4	13.9	0.7
chr9	Smarca4 (Brg)	20586	\SWI/SNF related, matrix associated, actin depender	-0.2	0.504	13.4	13.5	0.9
chr19	Smarca2 (Brm)	67155	\SWI/SNF related, matrix associated, actin depender	-0.1	0.827	13.6	13.6	1.0
chrX	Smarca1 Snf2L	93761	\SWI/SNF related, matrix associated, actin depender	-2.1	0.001	6.9	8.9	0.2
chr6	Chd4	107932	chromodomain helicase DNA binding protein 4	0.2	0.636	14.4	14.2	1.1
chr19	Ppp1ca	19045	\protein phosphatase 1, catalytic subunit, alpha isofo	-0.4	0.056	14.4	14.8	0.8
chr11	Ppp2ca	19052	\protein phosphatase 2 (formerly 2A), catalytic subur	0.0	0.924	12.7	12.7	1.0
chr7	Ppp4c	56420	\protein phosphatase 4, catalytic subunit\""	0.2	0.477	14.2	14.0	1.1
chr2	Ppp6c	67857	\protein phosphatase 6, catalytic subunit\""	0.5	0.057	13.4	12.9	1.4
chr11	Ppm1d (Wip1)	53892	\protein phosphatase 1D magnesium-dependent, del	0.0	0.924	10.0	10.0	1.0